^{63,65}Cu NMR Study of the Magnetically Ordered State of the Multiferroic $CuFeO_2$

Vasily V. Ogloblichev[1*)], Almaz F. Sadykov[1], Yuji Furukawa[2], Qing-Ping Ding[2], Alexey G. Smolnikov[1], Yuri V. Piskunov[1], Konstantin N. Mikhalev[1], Alexander P. Gerashenko[1], Anhua Wu[3], Sergei N. Barilo[4], Sergei V. Shiryaev[4]

[1]M.N. Miheev Institute of Metal Physics, Ural Branch, Russian Academy of Sciences, Yekaterinburg, 620108 Russia
[2]Ames Laboratory, Department of Physics and Astronomy, Iowa State University, Ames, IA 50011, USA
[3]Institute of Ceramic, Chinese Academy of Sciences, Shanghai 200050, People's Republic of China
[4]Institute of Solid State and Semiconductor Physics, National Academy of Sciences of Belarus, Minsk, 220072 Belarus
[*]*e-mail:* ogloblichev@imp.uran.ru

ABSTRACT

Field-swept ^{63,65}Cu NMR spectra under magnetic fields up to 8.3 T at a constant NMR frequency and temperatures T < 12 K on a single crystalline sample of multiferroic $CuFeO_2$ were measured and analyzed. When the magnetic field is applied along the *c* axis, a nearly zero internal magnetic field at the Cu site in magnetic ordered state was observed. This is explained by the perfect cancellation of the internal fields produced by the 6 nearest neighbor Fe^{3+} (S = 5/2) ions, revealing the magnetic structure to be a collinear four-sublattice structure. On the other hand, when the magnetic field is applied along the *ab* plane, we observed a finite internal field at the Cu sites, which is due to the canting of the Fe moments. Strong change in the NMR signal intensity is observed around 7-8 T, corresponding to the magnetic phase transition from the collinear magnetic to ferroelectric incommensurate states. The ratio of the two magnetic phases significantly depends on the history of the change in the external magnetic field and the temperature of the sample. The details of history dependence of the ratio were discussed.

Keywords: ^{63,65}Cu NMR; frustrated systems; collinear magnetic structure; delafossite structure.

INTRODUCTION

The research interest in $CuFeO_2$ delafossite is caused by the presence of a rich magnetic field(*H*)-temperature(*T*) phase diagram in this system. The competition of comparable exchange interactions in $CuFeO_2$ leads to spin frustration and the emergence of unusual examples of long-range and short-range magnetic orders [1-10]. In the zero external magnetic field, $CuFeO_2$ exhibits the magnetic phase transition from the paramagnetic phase (PM) to the partially disordered incommensurable (IC) magnetic phase (PDIC) at a temperature T_{N1} = 14 K. In the temperature range of 10.6 K < T < 14 K, a sinusoidal amplitude-modulated magnetic structure has been reported and the magnetic state was characterized by a temperature-dependent wave propagation vector (*q*, *q*, 0) [1-4]. Another magnetic phase transition at T_{N2} = 10.6 K brings the system to a four-sublattice collinear ground state (4SL) in which the iron spins align parallel to the *c* axis, forming a bidirectional two-row order (↑↑↓↓). One of the most intriguing properties of $CuFeO_2$ is the evolution of its magnetic structures when an external magnetic field is applied. It has been shown that with the direction of the magnetic field H along the *c* axis ($H \parallel c$), the material undergoes a series of magnetic transitions between phases with different types of magnetic ordering at a low temperature of T < 10.6 K: at 7 T < H < 13 T (a noncollinear incommensurate structure, the only magnetoelectrically active phase (FEIC)), 13 T < H < 20 T (collinear state 5SL (↑↑↑↓↓)), 20 T <

H < 34 T (collinear state 3SL (↑↑↓)), 34 T < H < 53 T (anisotropic canted spin configuration), H > 53 T (isotropic canted high-field magnetic order). When the magnetic field is applied in the *ab* plane, a series of magnetic transitions was also observed, but without the existence of a magnetoelectric phase [1-3,5,10].

Using ^{63,65}Cu nuclei as local nuclear magnetic resonance (NMR) probes allows us to obtain the information about spin exchange, local charge distribution and character of magnetic interaction between Fe^{3+} ions in neighboring planes [11,12]. In our previous works [13, 14] the paramagnetic phase of $CuFeO_2$ was investigated by ^{63,65}Cu NMR. It was shown that the temperature dependences of the NMR shifts of the ^{63,65}Cu NMR line $K(T)$ and the magnetic susceptibility $\chi(T)$ at T > 60 K are well described by Curie-Weiss law. But below $T \leq 60$ K, the behaviors of $K(T)$ and $\chi(T)$ are different. The deviation of $K(T)$ from the Curie-Weiss behavior indicates the development of antiferromagnetic spin correlations between iron planes in $CuFeO_2$ and/or the establishment of a near magnetic order below 60 K [13]. It was also shown that the main contribution to the ^{63,65}Cu NMR line shift is due to an isotropic field induced on the copper nucleus by electrons in partially occupied *S*-orbitals through contact Fermi hyperfine interaction. The anisotropic contribution to the ^{63,65}Cu NMR line shift originates from spin-dipole and hyperfine interactions with the electrons in the 3*d* orbital, as well as the dipole interaction of the nucleus with the magnetic moments of neighboring Fe^{3+} ions [14].

The aim of this work is to study the magnetic properties in the magnetically ordered state in $CuFeO_2$ and its evolution on the magnetic field and temperature from a microscopic point of view by using nuclear magnetic resonance technique. This paper reports NMR data of a $CuFeO_2$ single crystal in the temperature range T = 1.6-12 K in the magnetic fields up to 8.3 T.

SAMPLES AND METHODS OF THE EXPERIMENT

The $CuFeO_2$ samples studied in this work were single crystals with dimensions of 2×2×1 mm. The method of sample preparation is described in detail in Ref. [13].

X-ray diffraction analysis of powdered crystals showed that $CuFeO_2$ has a rhombohedral crystal structure with symmetry $R\bar{3}m$ with unit cell parameters a = 3.031(1) Å and c = 17.162(2) Å at room temperature. These data are in agreement with those previously obtained in Refs. [15-17] and were used to calculate the dipole fields presented in the following section.

NMR study was carried out on a homemade spectrometer with a superconducting magnet (Oxford Instruments) with the ability to scan the magnetic field from 0 to 8.3 T. In all experiments stabilization and measurement of the sample temperature was carried out with an accuracy of 0.05 K by using two temperature controllers ITC 5 (Oxford Instruments) controlling the temperatures of the cryostat heat exchanger and the resonance cell in the vicinity of the sample.

NMR spectra of ^{63,65}Cu were obtained using the standard pulse sequence τ–t_{del}–2τ–t_{del}–*echo* in the magnetic field sweep mode at irradiation frequencies of ν_0 = 57, 64, and 76 MHz. The duration of the first pulse was selected $\tau \approx 1$ μs. The repetition time of the pulse sequence was 50 ms. Measurements of NMR spectra were carried out at delays between pulses of t_{del} = 8 - 15 μs.

The spin-spin relaxation time T_2 was measured by changing the delay between pulses in the pulse sequence in the interval t_{del} = 8 - 100 μs.

To calculate the shape and shift of the NMR lines, the simulation program of NMR spectra (Simul) was used, in which the shapes of the NMR lines were calculated numerically based on the full Hamiltonian of the nuclear system taking into account the interaction of the quadrupole moment of the nucleus with the electric field gradient (EFG) of the environment, dipole-dipole and hyperfine interactions [18-20].

RESULTS AND DISCUSSION

The observed ^{63,65}Cu NMR signals in the paramagnetic phase of $CuFeO_2$ are characterized by very short spin-spin relaxation time $T_2 \approx 5$ μs and spin-lattice relaxation time $T_1 < 100$ μs [13,14]. In the temperature range of 10.6 K < T < 14 K, corresponding to the PDIC phase, the NMR signal of ^{63,65}Cu, unfortunately, could not be observed. The main reason for the lack of a signal is most likely due to a further shortening of the spin-spin relaxation time. On the other hand, the ^{63,65}Cu NMR signals were observed in the magnetically ordered phase below $T_{N2} = 10.6$ K. It was found an exponential increase in spin-spin relaxation time as the temperature decreases: from $T_2 = 10$ μs at $T = 10$ K to $T_2 = 80$ μs at $T = 1.6$ K.

Figure 1 shows the typical field-swept ^{63,65}Cu NMR spectra measured at $T = 1.68$ K and a frequency of $\nu_0 = 57$ MHz for two orientations of the external magnetic field, $H \parallel c$ and $H \parallel ab$ ($H \parallel [\bar{1}10]$)**.** The ^{63,65}Cu NMR spectra ($I = 3/2$) of the $CuFeO_2$ single crystal represent two sets of lines corresponding to ^{63}Cu and ^{65}Cu isotopes with gyromagnetic ratios of $^{63}\gamma/2\pi = 11.28$ MHz/T and $^{65}\gamma/2\pi = 12.09$ MHz/T respectively. The NMR signal intensities of ^{63}Cu and ^{65}Cu correspond to their natural abundances of 69% and 31%, respectively. The NMR spectrum of each isotope consists of three lines: the central one corresponding to the transition $m_I = 1/2 \leftrightarrow -1/2$, and two satellites - transitions $m_I = -3/2 \leftrightarrow -1/2$ and $m_I = 1/2 \leftrightarrow 3/2$. The appearance of the satellite lines is caused by the interaction of the quadrupole moments of ^{63}Cu and ^{65}Cu nuclei ($e^{63}Q = 0.220\times10^{-24}$ cm^2, $e^{65}Q = 0.204\times10^{-24}$ cm^2) with the electric field gradient (EFG) created at the location of the nuclei by their charge environment [21]. Narrow lines on NMR spectra near zero shift are associated with signals from ^{63}Cu and ^{65}Cu isotopes in copper metals contained in the resonance circuit.

It was established in our previous work [13] that the main EFG-axis in the paramagnetic phase of $CuFeO_2$ is directed along the c-axis of the crystal, the tensor EFG has axial symmetry $V_{XX} \approx V_{YY} \approx 0.5V_{ZZ}$ with the asymmetry parameter $\eta = (V_{XX} - V_{YY})/V_{ZZ} \approx 0$ and the values of the quadrupole frequencies are $^{63}\nu_Q = e^{63}Q\cdot V_{ZZ}/2h = 26.6(4)$ MHz and $^{65}\nu_Q = e^{65}Q\cdot V_{ZZ}/2h = 24.6(7)$ MHz. From the analysis of the NMR spectra observed in the magnetically ordered phase, the following EFG tensor components were obtained: $^{63}\nu_Q = 26.6(5)$ MHz, $^{65}\nu_Q = 24.6(8)$ MHz, and $\eta \approx 0$. In the structure of $CuFeO_2$, the EFG tensor on the copper nuclei is determined mainly by its nearest charge environment, which includes two oxygen ions O^{2-}, forming a linear chain O – Cu – O along the c axis of the crystal (Fig. 2). The coincidence of quadrupole frequencies in the paramagnetic [14] and magnetically ordered phases indicates that the local charge environment of copper nuclei (mutual arrangement of copper and oxygen ions) does not change during the magnetic phase transition. A similar constancy of the EFG parameters at the copper nuclei was found in the isostructural $CuCrO_2$ [22].

It is noted that the relative intensities of the central line and the quadrupolar satellites in the observed spectrum are different from those in the simulated spectrum. The difference in the ^{63,65}Cu NMR line intensities is due to spin-spin relaxation times which are not the same in different positions of the NMR spectrum. For example, the spin-spin relaxation time (T_2) for satellite lines ($^{63,65}m_I = -3/2 \leftrightarrow -1/2$, left satellites) is about 71 μs, for central transitions ($^{63,65}m = -1/2 \leftrightarrow 1/2$) $T_2 \approx 42$ μs, for other satellite lines ($^{63,65}m_I = 3/2 \leftrightarrow ½$, right satellites) $T_2 \approx 32$ μs at $T = 1.68$ K. We consider that the difference in spin-spin relaxation behavior relates to the proximity to the 4SL↔FEIC transition. Another factor that affects the intensity of lines may be the coexistence of the 4SL and FEIC phases in the high field region, as discussed below.

Copper ions in the $CuFeO_2$ structure are located between two adjacent planes containing Fe^{3+} ions as shown in Fig. 2. In general, the local field at the non-magnetic copper ion is determined by both the dipole field H_{dip} generated by the magnetic moments of Fe^{3+} ions and the hyperfine field H_{hf}, associated with the transfer of spin polarization from the nearest magnetic neighbors:

$$\mathbf{H}_{\rm loc} = \mathbf{H}_{\rm dip} + \mathbf{H}_{\rm hf} = \sum_i (\boldsymbol{h}_{dip,i} + \boldsymbol{h}_{hf,i}). \quad (1)$$

Here, $h_{{\rm dip},i}$ and $h_{{\rm hf},i}$ are local dipole and hyperfine fields on copper ions, which were produced by Fe^{3+} ions on *i*-position in crystal lattice. The main contribution to the induced field on the copper site in the paramagnetic phase is an isotropic hyperfine field with a constant A_{iso} = 2.08 T/μ_B [13]. At $T >> T_{N1}$ in the absence of correlations between the magnetic moments of iron, the resulting hyperfine field on copper nuclei is directed along the external magnetic field and is equal in magnitude to the sum of the hyperfine fields from each of the 6 nearest Fe^{3+} ions:

$$\mathbf{H}_{\rm hf} = \sum_{i=1}^{6} \mathbf{h}_{hf,i} = \sum_{i=1}^{6} \mathrm{A}_{iso}^{i} \boldsymbol{\mu}_i. \quad (2)$$

Here μ_i is the magnetic moment of iron ion on *i*-position. The Fe^{3+} ions in $CuFeO_2$ are in the high spin state S= 5/2 ($3d^5$), and the magnetic moment of Fe^{3+} is reported to be 4.0-4.20 μ_B from the neutron diffraction measurements [1,5]. Using the value μ = 4.20 μ_B [5], we estimate that one Fe^{3+} ion creates a field on the copper nucleus $h_{{\rm hf},1} = A_{iso} \times \mu/6$ =1.456 T.

Now let us consider the details of the magnetic structure in an ideal 4SL (↑↑↓↓) state. There are fundamentally two different configurations of Fe spins relative to the copper ion as shown in Figs. 2a and 2b.

The first spin configuration involves the Fe planes, in which four Fe^{3+} ions out of six compensate for their induced hyperfine fields on the copper ion, and the other two do not. Figure 2a shows an example of such a configuration ↓↑↑/Cu/↓↑↑, where the order of the arrows corresponds to the numbers of Fe atoms 123/Cu/456. The magnitude of the induced hyperfine field on the copper ion from two Fe^{3+} ions is equal to $H_{\rm hf} = \mu\, 2\, h_{{\rm hf},1} \approx \pm 2.92$ T. This finite hyperfine fields will result in two symmetrically NMR lines split by $\pm H_{\rm hf}$ for each copper isotope line relative to the zero shift value K = 0. This is not observed in the experiment and, therefore, this configuration of the Fe magnetic moments relative to copper ions ↓↑↑/Cu/↓↑↑ is not consistent with the observed NMR spectra.

The second possible configuration of the Fe^{3+} magnetic moments with respect to the copper ion is ↓↑↑/Cu/↑↓↓ shown in Fig. 2b. In such a structure, the total induced hyperfine field at the copper ion from the Fe^{3+} ions is completely cancelled out (i.e., $H_{\rm hf}$ = 0). In this case, the ^{63,65}Cu NMR line shift will be determined only by the dipole fields (eq. 1). The calculation of dipole fields at the Cu site was carried out within the three coordination spheres using the usual expression:

$$\mathbf{H}_{\rm dip} = \sum_i (3\mathbf{r}_i(\boldsymbol{\mu}_i \mathbf{r}_i) - \boldsymbol{\mu} \mathbf{r}_i^2)/\mathbf{r}_i^5 \quad , \quad (3)$$

where $r_i^2 = (x^2 + y^2 + z^2)$ is the square of the distance Cu–Fe_i; μ_i – is the magnetic moment of the iron ion in the crystallographic position with coordinates (*x*, *y*, *z*). From the calculation, we found that the maximum projection of the dipolar field is along the *a* axis with $h_{\rm dip}^a \sim 0.45$ T and the dipolar field along the *c* axis is nearly zero ($h_{\rm dip}^c \sim 0$ T). The dipolar field on the copper ions along the crystallographic *c* axis in the 4SL phase is nearly zero, therefore, the shift of the ^{63,65}Cu NMR in $H \parallel c$ should be close to zero, which is actually observed in the experiment. On the other hand, when *H* is applied along the *ab* plane, the dipole field $h_{\rm dip}^a \sim 0.45$ T leads to a Gaussian broadening of the ^{63,65}Cu NMR spectra. The dashed lines in Fig. 3 show the simulated spectra using the aforementioned dipolar fields. As can be seen, the observed ^{63,65}Cu NMR spectra are well reproduced by the simulations for both $H \parallel c$ and $H \parallel ab$. Therefore, we conclude that the local magnetic configuration is given by ↓↑↑/Cu/↑↓↓.

Now we discuss the NMR shift of the ^{63,65}Cu NMR spectra for $H \parallel ab$. The shift is associated with the second-order quadrupole correction [18,19,21] and the canting of the magnetic moments along the magnetic field. The presence of such canting in magnetic fields of 0-25 T in the direction $H \perp c$ has been indicated previously [3,5]. The induced hyperfine fields on the copper ion are

uncompensated in the case of canting of the iron magnetic moments, leading to an additional local field H_{loc}^{ab} (the inset in Fig. 3b).

Figure 3a shows field-swept ^{63,65}Cu NMR spectra obtained at T = 1.68 K and at frequencies ν_0 = 57, 64 and 76 MHz for $H \parallel ab$. By simulating each experimental NMR spectrum, H_{loc}^{ab} values were estimated. The local fields H_{loc}^{ab} at the ^{63}Cu and ^{65}Cu sites are given in Fig. 3b (right scale). The obtained H_{loc}^{ab} are well approximated by the dependence $H_{loc}^{ab} = 0.11(2)\times H$. Using the known value of the hyperfine interaction constant A_{iso} and the local field H_{loc}^{ab}, it is possible to estimate the angle of the canting of the magnetic sublattice of iron ions (Θ):

$$\mathrm{Sin}\,(\Theta) = H_{loc}^{ab}/\mu A_{iso} \qquad (4)$$

Figure 3b (left scale) shows the dependence of the angle Θ on the external magnetic field H applied along the *ab* plane of the crystal. It is shown that the obtained data are well approximated by Θ = arcsin(0.013(3)×H).

In H = 7.0 - 8.0 T for $H \parallel c$ [1,2,3], the material undergoes a magnetic transition from the 4SL phase to the noncollinear incommensurate structure (FEIC) phase. An important point for the magnetic transition is whether external magnetic field is applied or not when the sample is cooled down passing the magnetic phase transition. As shown in Fig. 4, the ^{63,65}Cu NMR spectra significantly depend on the conditions of the transition to the magnetically ordered state from the paramagnetic state. The upper two ^{63,65}Cu NMR spectra were obtained by cooling the sample to T = 4.2 K in a zero external magnetic field and scanning the field first in the direction of increasing the magnetic field to H = 8.3 T (upper spectrum), then in the direction of decreasing to H = 0 (middle spectrum). There is a significant difference in the intensities of high-field satellites for those spectra. When the spectra obtained by cooling the sample in a magnetic field H = 8.3 T (bottom spectrum), satellite lines in the H region of 6.5 - 7.5 T are not observed at all. This is probably due to short spin-spin relaxation times of the NMR signals in the FEIC phase, making the observation difficult. Note that signals observed below 5 T (see the bottom spectrum) are assigned to those originated from the 4SL phase.

The inset in Fig. 4 shows the dependence of the intensity of the satellite ^{65}Cu NMR line transition $^{65}m_I = 3/2 \leftrightarrow 1/2$ on the magnitude of the magnetic field during its cycling. The cycling of the magnetic field was carried out in two stages as follows. In the first stage (blue squares), the sample was cooled to T = 4.2 K in a zero external magnetic field. After cooling, the ^{63,65}Cu NMR spectrum was recorded after the magnetic field was increased from 0 to 8.3 T. Then the magnetic field was lowered to H = 6.7 T and the signal intensity of the ^{65}Cu NMR satellite line was recorded. Then, followed the reduction of the field to a certain value (H_C = 6.25, 6, 5.5, 5 T, etc.), we measured the signal intensity of the ^{65}Cu NMR high-field satellite at H = 6.7 T. Here it is important to note that the intensity is proportional to the amount of the 4SL phase in the sample. The intensity is plotted as a function of H_C in the inset of Fig. 4. The intensity of the ^{65}Cu NMR line recovers to a maximum intensity only when H_C is less than 2.5 T.

In the second stage (red circles on the inset of Fig. 4), the sample was cooled to T = 4.2 K in a zero external magnetic field. After that, the magnetic field was increased from zero to H = 6.7 T, at which the intensity of the ^{65}Cu NMR signal $^{65}m_I = 3/2 \leftrightarrow 1/2$ was recorded. This gives the maximum intensity corresponding to the case that the all sample is in 4SL phase. To see how much the 4SL phase changes to the FEIC phase by increasing magnetic field, we increase the magnetic field up to H_C (for example, H_C = 7 T) and then decrease H down to 6.7 T where the signal intensity was measured. We repeated this cycle with different H_C and found the intensity starts to decrease drastically around H_C ~7.5 T. The intensity is suppressed down to ~ 10% of the maximum intensity around 8.2 T. The decrease in the NMR signal intensity corresponds to the magnetic phase transition from the 4SL to FEIC magnetic phases.

The obtained results indicate the existence of the hysteresis expected for the first order phase transition between 4SL and FEIC magnetic states. In H = 2.5-8.0 T, the two phases (4SL

and FEIC) can coexist. This fact is confirmed by the data on magnetization [1-4]. Interestingly the hysteresis loop is asymmetric and the slope depends on the field when it cycles in the directions of increase and decrease (see the inset in Fig. 4). At present, we do not have any clear idea to explain the different slopes. Further detail studies such as similar measurements at different temperature will be needed to clarify the origin of the asymmetric hysteresis loops for the 4SL-FEIC magnetic phase transition.

CONCLUSION

We have carried out ^{63,65}Cu NMR spectrum measurements on the $CuFeO_2$ single crystal in the collinear four sublattices (4SL) magnetically ordering state. When the magnetic field was applied along the *c* axis, it is found that the induced hyperfine fields at the copper site are near zero. Based on the observation of the zero internal field, the magnetic structure of the 4SL state was determined. On the other hand, when the magnetic field is applied along the *ab* plane, the finite internal field at the Cu site was observed, which is due to the canting of the Fe^{3+} magnetic moments. By measuring the external field dependence of the internal field, we estimated the magnetic field dependence of the canting angle of Fe^{3+} magnetic moments from the *c* axis. It is also shown that the transition from paramagnetic to magnetically ordered phase in the $CuFeO_2$ crystal preserves the linear configuration of O – Cu – O chains. The transition from 4SL to FEIC magnetic states depends on the history of cooling of the sample and of the applied magnetic field. The two phases (4SL and FEIC) can coexist in the region of H = 2.5-8.0 T at T = 1.68 K. The clear observation of the hysteresis of NMR signal intensities due to the transition between the 4SL and FEIC magnetic state indicates the magnetic phase transition is characterized by a first order magnetic phase transition.

ACKNOWLEDGMENTS

The research was carried out within the state assignment of Minobrnauki of Russia (theme “Function” No. AAAA-A19-119012990095-0). A.S. are grateful to the administration staff of the Ames Laboratory and Iowa State University for hospitality and support. The research was supported by the US Department of Energy, Office of Basic Energy Sciences, Division of Materials Sciences and Engineering. Ames Laboratory is operated for the US Department of Energy by Iowa State University under Contract No. DE-AC02-07CH11358. The work in Minsk and Shanghai was supported in part by BRFFI-NFENK grant #F18K-022. Anhua Wu thanks for the support from the Science and Technology Commission of Shanghai Municipality (No.19520710900)

LITERATURE

[1] M. Mekata, N. Yaguchi, T. Takagi, S. Mitsuda, H. Yoshizawa. Journal of Magnetism and Magnetic Materials **104-107**, 823 (1992).
[2] G. Quirion, M. L. Plumer, O. A. Petrenko, G. Balakrishnan, C. Proust. Physical Review B **80**, 064420 (2009).
[3] T.T. A. Lummen, C. Strohm, H. Rakoto, P. H. M. van Loosdrecht. Physical Review B **81**, 224420 (2010).
[4] O.A. Petrenko, M.R. Lees, G. Balakrishnan, S. de Brion, G. Chouteau. Journal of Physics: Condensed Matter **17**, 2741 (2005).
[5] Zuo Hua-Kun, Shi Li-Ran, Xia Zheng-Cai, Huang Jun-Wei, Chen Bo-Rong, Jin Zhao, Wei Meng, Ouyang Zhong-Wen and Cheng Gang. Chinese Physics Letters **32(4)**, 047502 (2015).
[6] F. Ye, Y. Ren, Q. Huang, J.A. Fernandez-Baca, Pengcheng Dai, J.W. Lynn, T. Kimura. Physical Review B **73**, 220404R (2006).
[7] T. Nakajima, S. Mitsuda, K. Takahashi, M. Yamano, K. Masuda, H. Yamazaki, K. Prokes, K. Kiefer, S. Gerischer, N. Terada, H. Kitazawa, M. Matsuda, K. Kakurai, H. Kimura, Y. Noda, M. Soda, M. Matsuura, K. Hirota. Physical Review B **79**, 214423 (2009).
[8] S. Nakamura, Y. Kobayashi, S. Kitao, M. Seto, A. Fuwa, N. Terada. Journal of the Physical Society of Japan **84**, 024719 (2015).
[9] S. Mitsuda, M. Mase, K. Prokes, H. Kitazawa, H. A. Katori. Journal of the Physical Society of Japan **69**, 3513 (2000).
[10] H. Tamatsukuri, S. Mitsuda, T. Shimizu, M. Fujihala, H. Yokota, K. Takehana, Y. Imanaka, A. Nakao, K. Munakata. Physical Review B **100**, 201105(R) (2019).
[11] R.Nath, R.M. Ranjith, B. Roy, D.C. Johnston, Y. Furukawa, A.A. Tsirlin. Physical Review B **90**, 024431 (2014)
[12] V. Ogloblichev, K. Kumagai, S. Verkhovskii, A. Yakubovsky, K. Mikhalev, Y. Furukawa, A. Gerashenko, A. Smolnikov, S. Barilo, G. Bychkov, and S. Shiryaev. Physical Review B **81**, 144404 (2010).
[13] V.V. Ogloblichev, A.G. Smolnikov, A.Yu. Germov, Y.V. Piskunov, A.F. Sadykov, K.N. Mikhalev, A.Yu. Yakubovsky, S.N. Barilo, S.V. Shiryaev. Applied Magnetic Resonance **50**, 371 (2019).
[14] A.G. Smol'nikov, V.V. Ogloblichev, A.Yu. Germov, K.N. Mikhalev, A.F. Sadykov, Yu.V. Piskunov, A.P. Gerashchenko, A.Yu. Yakubovskii, M.A. Muflikhonova, S.N. Barilo, S.V. Shiryaev. Journal of Experimental and Theoretical Physics Letters **107**, 134 (2018).
[15] T. Kimura, J.C. Lashley, A.P. Ramirez. Physical Review B **73**, 220401 (2006).
[16] P. Dordor, J.P. Chaminade, A. Wichainchai, E. Marquestaut, J.P. Doumerc, M. Pouchard, P. Hagenmuller. Journal of Solid State Chemistry, **75**, 105 (1988).
[17] T-R. Zhao, M. Hasegawa, H. Takei. Journal of Crystal Growth, **154**, 322 (1995).
[18] A.F. Sadykov, A.P. Gerashchenko, Yu.V. Piskunov, V.V. Ogloblichev, A.G. Smol'nikov, S.V. Verkhovskii, A.Yu. Yakubovskii, E.A. Tishchenko, A.A. Bush. Journal of Experimental and Theoretical Physics **115**, 666 (2012).
[19] A.G. Smol'nikov, V.V. Ogloblichev, S.V. Verkhovskii, K.N. Mikhalev, A.Yu. Yakubovskii, Y. Furukawa, Yu.V. Piskunov, A.F. Sadykov, S.N. Barilo, S.V. Shiryaev. Physics of Metals and Metallography **118**, 134 (2017).
[20] A.G. Smol'nikov, V.V. Ogloblichev, S.V. Verkhovskii, K.N. Mikhalev, A.Yu. Yakubovskii, K. Kumagai, Y. Furukawa, A.F. Sadykov, Yu.V. Piskunov, A.P. Gerashchenko, S.N. Barilo, S.V. Shiryaev. Journal of Experimental and Theoretical Physics Letters **102**, 674 (2015).
[21] C.P. Slichter. *Principles of Magnetic Resonance*. New York: Harper & Row, 1963. 246 p.
[22] A. Smolnikov, I. Arapova, V. Ogloblichev, Yu. Piskunov, A. Sadykov, K. Mikhalev, Y. Furukawa, S. Barilo, S. Shiryaev. Journal of Physics: Conference Series **1389**, 012136 (2019).

Figure captions

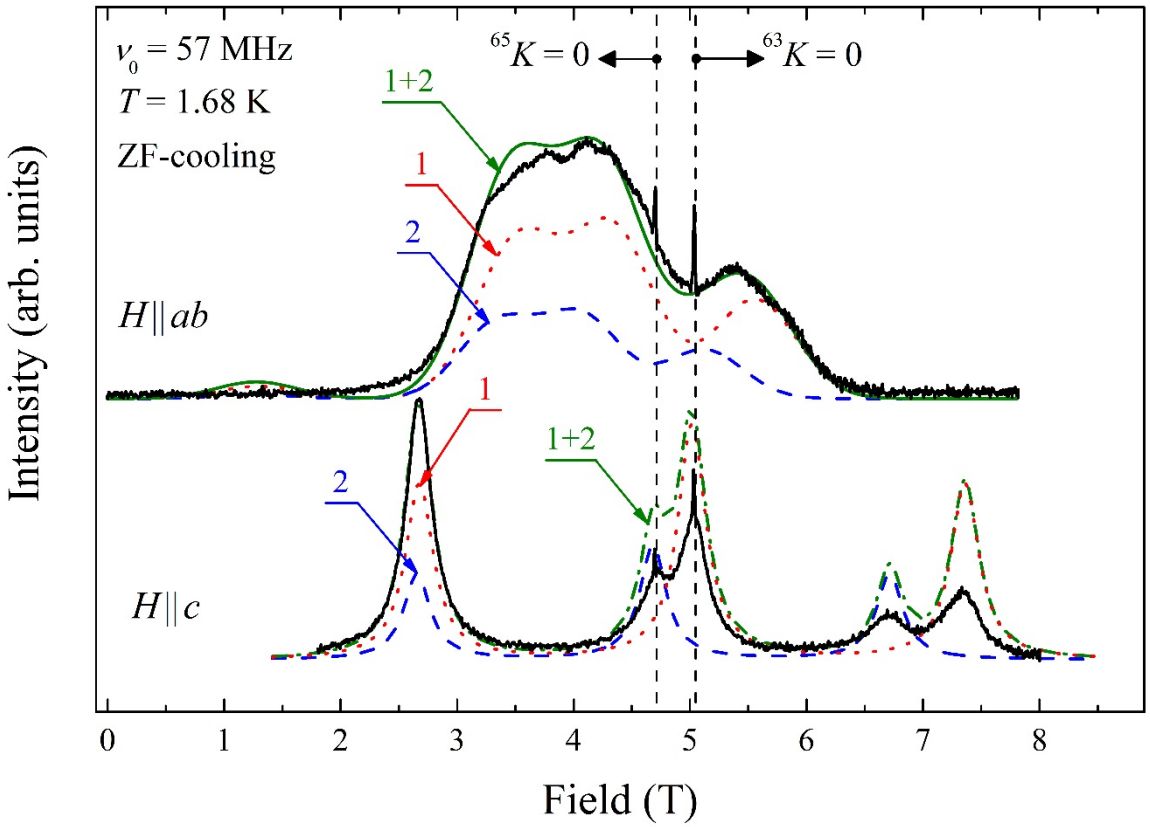

Fig.1. ^{63,65}Cu NMR spectra of $CuFeO_2$ single crystal measured at magnetic field orientations $H \parallel c$ and $H \parallel ab$ (H||[$\bar{1}$10]) in the magnetically ordered phase 4SL, T = 1.68 K and ν_0 = 57 MHz. The dashed lines are the result of spectrum modeling: line 1 corresponds to the copper isotope ^{63}Cu, line 2 to ^{65}Cu, line 1+2 to the total spectrum of lines 1 and 2.

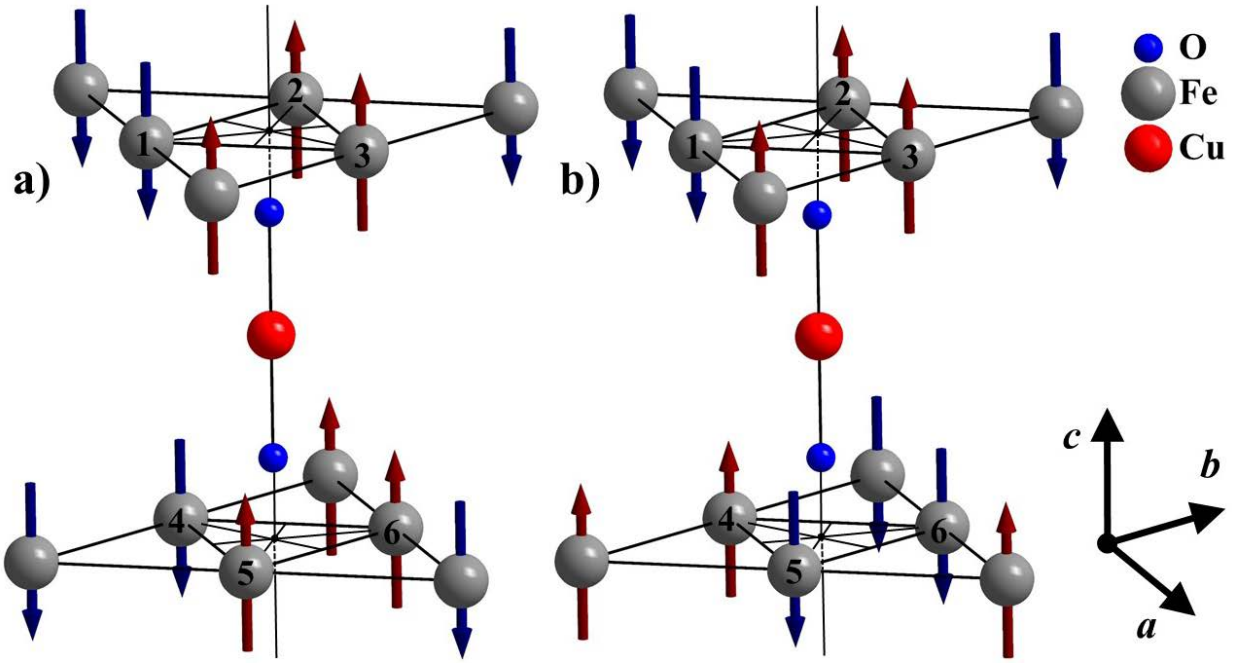

Fig.2. Image of possible magnetic structures in the magnetically ordered phase 4SL. Two planes of Fe^{3+} magnetic moments in the first coordination sphere with incomplete {↓↑↑/Cu/↓↑↑}-(a) and full {↓↑↑/Cu/↑↓↓}-(b) cancellations of the induced hyperfine field on the copper ion. The order of the arrows in the designations corresponds to the numbers of iron atoms {123/Cu/456}. The line passing through the O – Cu – O chain intersects the planes of iron ions in the center of an equilateral triangle.

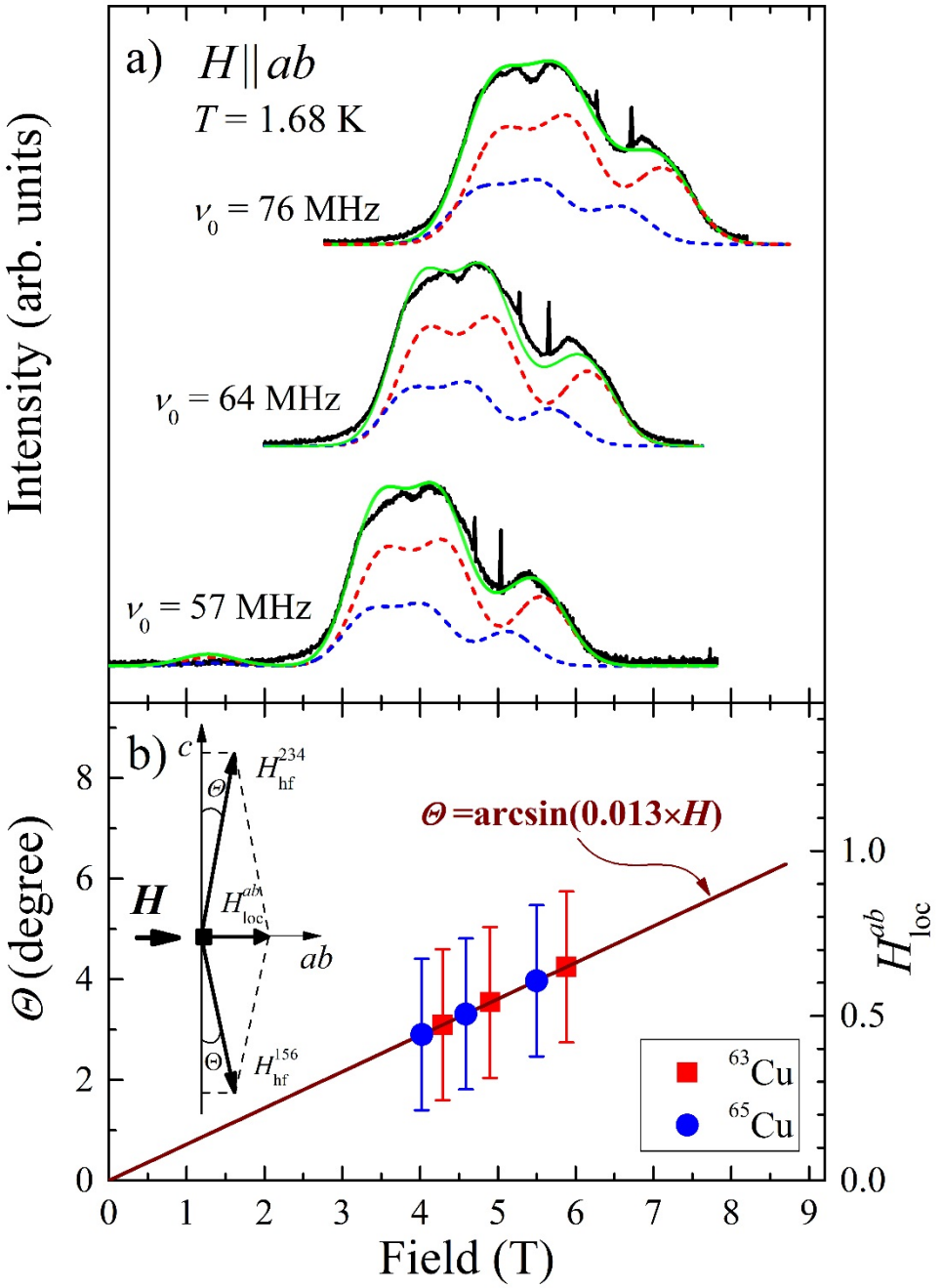

Fig. 3. (a) Field-swept ^{63,65}Cu NMR spectra measured at frequencies ν_0 = 57; 64; 76 MHz at $H \parallel ab$ and T = 1.68 K. Dashed lines are the result of spectrum modeling (by analogy with Fig.1). (b) The angle of deflection Θ of the hyperfine field H_{hf} induced by magnetic moments of iron 1,2,3,4,5,and 6 (Fig. 2) on copper ions, depending on the applied magnetic field along the *ab*-plane.

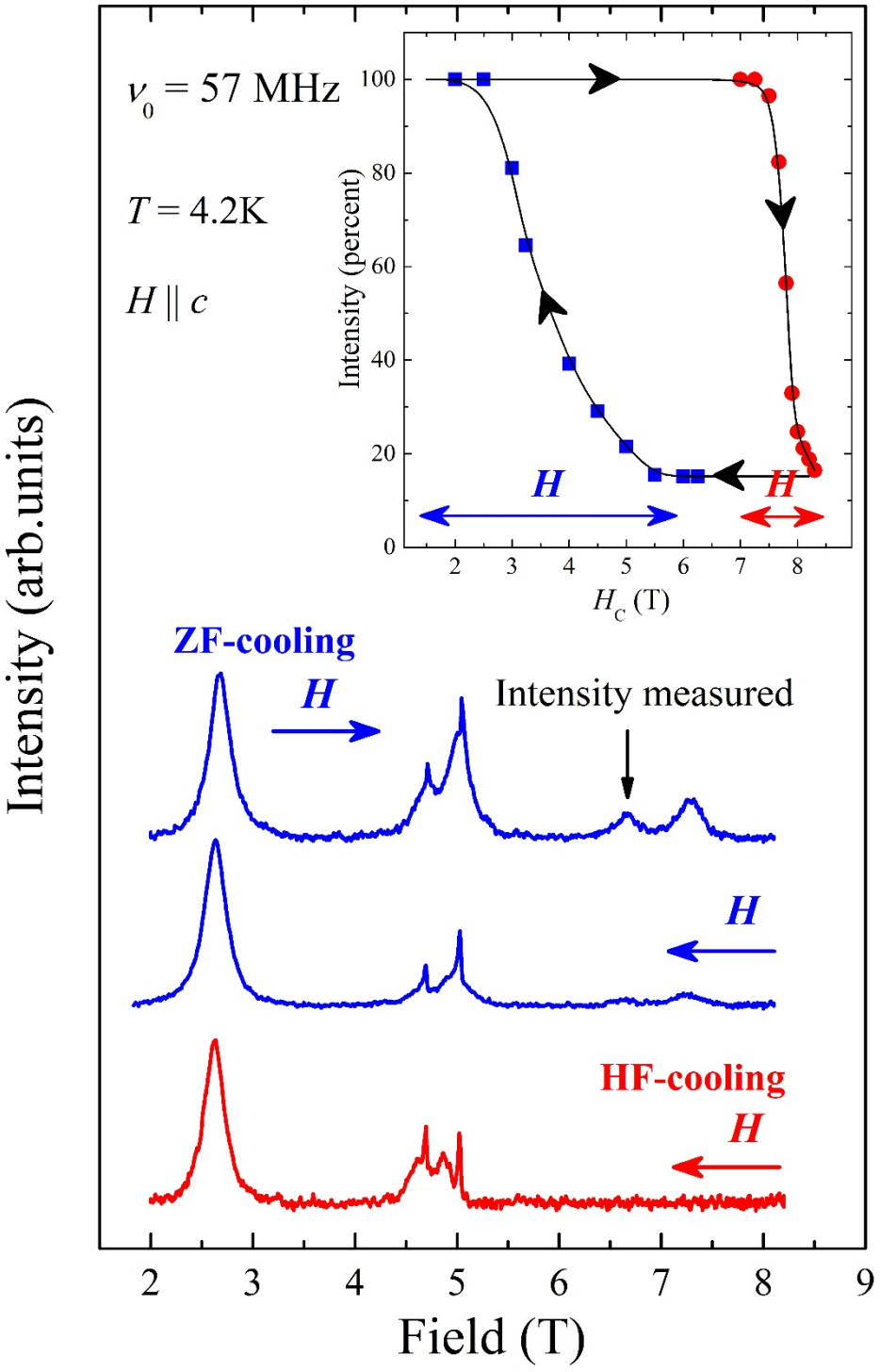

Fig.4. Field-swept ^{63,65}Cu NMR spectra measured at a frequency of ν_0= 57 MHz under the magnetic field $H \parallel c$ with the cooling of the $CuFeO_2$ sample to a temperature T = 4.2 K without and in an external magnetic field. The inset presents the dependence of the intensity of the ^{65}Cu NMR transition $^{65}m_I = 3/2 \leftrightarrow 1/2$ on the value of the cycling magnetic field H_C (see text).